



Experimental and Numerical Evaluation for Bearing Capacity of a Square Footing on Geotextile Reinforced Sandy Soil

Hussein Shaia^(✉) and Lubna Thamer

Civil Engineering Department, University of Thi-Qar, Thi-Qar, Iraq
h.shaia@utq.edu.iq

Abstract. The technique of strengthened soil is a composite material made up of high tensile strength materials are included to enhance the tensile strength of the soil. Geotextile was utilized to strengthen the soil. The model footing was constructed from a steel plate measuring 100 mm by 100 mm. The top layer spacing and the number of reinforcing layers were examined in this research. Additionally, the scale effect of model testing was numerically investigated by conducting a three-dimensional finite element analysis using (ABAQUS) on various sizes of square footing. Also, the impact of geotextile thickness and the behavior of sand on top of silty sand with three woven geotextiles on ultimate bearing capacity (BC) was studied. The experimental findings indicate that the system with three geotextile layers, and a top layer spacing of 0.25 B, where B is (the plate's width), achieves the maximum bearing capacity. The numerical analyses indicated that the BCR decreases as the footing size increases (B). Also, it should be noted that as the thickness of the geotextile increases, the bearing capacity (BC) of the soil increases. A good agreement between the experimental and numerical results was observed when the numerical analysis findings were compared to those obtained from experimental investigations.

Keywords: Bearing capacity · BCR · Square footing · Geotextile · ABAQUS · Finite element analysis

1 Introduction

Footings are built on weak soil deposits with low or medium plasticity, resulting in inadequate BC and significant settlement concerns. This may result in structural failure, decreased durability, and/or reduced performance. Traditional treatment techniques included replacing a portion of the poor soil with a sufficiently thick layer of stronger granular fill, enlarging the footing, or combining the two. However, one of the more cost-effective options is strengthening soils using geotextile materials. This may be accomplished by directly supporting the soil or replacing it with a stronger granular fill combined with geotextile. The resultant composite zone will increase the footing's load BC and improve pressure distribution across the underlying weak soils, thus minimizing related settlements. It is a highly cost-effective method for avoiding the need for costly

deep foundations [1]. Sandy soils may be found throughout the world, and they are increasingly being utilized for building. However, several issues are related to the usage of sandy soils in construction, such as slope stability, foundation bearing capacity, and liquefaction.

Many strategies were developed to address these issues and improve ground quality. Among these measures, reinforcing soil under the foundation is common to increase bearing capacity and decrease foundation settlement. The basic aims of soil reinforcement are decreasing settlements and lateral deformation, enhancing stability, and increasing capacity. Geosynthetics are produced from different polymers and are employed to perform the following activities: separation, reinforcing, filtration, and drainage. Geotextile is the most popular geosynthetics [2]. Many studies have looked at the benefits of using geosynthetic soil strengthening. Banquet and Lee conducted the first comprehensive investigation into using metallic strips to increase strip footing BC [3]. After that, many analyses have been conducted to understand better the behavior of reinforced soil bases and the influence of different conditions on their BC, including [4–10]. Yetimoglu et al. investigated the carrying capacity of footings on sandy soil strengthened by one layer of geogrid and showed that $0.3 B$ is the best reinforcing depth [11].

Sitharam and Sireesh [12] tested a laboratory model of sand-supporting circular footing reinforced with numerous geogrid layers to assess its bearing capacity. The tests showed that when the embedment depth ratio of a foundation grows, the maximum bearing pressure also improves. Latha & Somwanshi investigated the BC of geosynthetic-reinforced sand footing and the effect of various reinforcement variables. The tests show that the effective reinforcement depth was $2 B$; the appropriate spacing of geosynthetic layers is $1/2 B$ (B is the width of the footing). They also carried out a numerical study to evaluate the influence of reinforcing agent form [13]. Abu-Farsakh et al. used several experimental tests to investigate the impact of various characteristics relating to their efficiency. They used three distinct kinds of geogrids and one type of geotextile. The experimental results showed that the reinforcing arrangement had a substantial impact on the activities of the upgraded sand foundation. Sand reinforced using geogrids and geotextiles performed better than geogrids or geotextiles reinforced alone [14].

Kazi et al. [15] contrasted the experimental findings for laboratory model strip load experiments, focusing on sand beds supported by a single sheet of woven geotextile reinforcement with wrap-around ends, with numerical findings focused on the finite element model conducted using the PLAXIS 2D program (version 9.0). The findings indicate that the suggested approach of wrapping around the ends of geosynthetic reinforcement improves the overall capacity of load BC. A substantial improvement in the stiffness of a sand sheet in respect of the modulus of subgrade reaction and gains inland area for the development of a strengthened sand bed structure. Tavangar & Shooshpasha evaluated the effects of utilizing nonwoven geotextile to raise the maximum BC of shallow foundations on medium-density sand. In addition, the numerical influence of footing size and the sample size was investigated by running finite element calculations with varied sizes of square plates. According to their results, the system with a $0.3 B$ vertical separation between geotextile and four geotextile layers had the greatest bearing capacity. The numerical investigations revealed that raising the footing size up to 65 cm decreases

the bearing capacity ratio values; however, any further rise in plate size has a negligible influence on the BCR values [16].

Geo jute has been utilized as a geotextile by Panigrahi and Pradhan to boost soil carrying capacity. According to the results of the trials, the most effective depth was found at 0.5 B. The largest advantage was obtained at the optimal reinforcing size of 3.5 B by 3.5 B, irrespective of the size of the footing. The findings of laboratory model testing and numerical studies on square footings supported by sand with and without geotextile strengthening are reviewed in this work [17]. The major goal of this research is to determine the effectiveness of geotextile layers in improving the BC of square footings and the influence of different reinforcing parameters on total footing performance improvements. The model tests consider the top layer spacing (u) and the number of reinforcement layers (N). Additionally, it has been examined. The size impact of model footing test findings, the thickness of geotextile layers, and determine the advantage of using a thin layer of sand over silty sand soil to increase the soil's bearing capacity by using the 3-D finite element analyses program ABAQUS.

2 Laboratory Setup and Materials of the Est

Figure 1 depicts the experimental setup used in this work. The system comprises a (600 × 600 × 400) mm length, width, and height. The plates that constitute the box's bottom and sides are six mm thick, creating them strong enough to withstand the loading stresses. The container's foundation is made of solid steel and is 800 mm wide by 1100 mm long. It is coupled to a loading frame. The steel box is constructed from six mm steel plates bolted together and welded to a 75 by 75 and 6 mm steel angle. Two columns plus a loading platform make up the loading frame. Additionally, (100 × 100) mm square plates with a thickness of 20 mm were employed in this investigation. The foundation was set such that the middle of the footing corresponded with the middle of the soil and was in touch with the ground's top surface. These measurements were established in accordance with the (ASTMD-1194) plate standard. The settling of the footing must be determined using two dial gauges mounted on reference beams having a measurement range of 25 mm and an accuracy of 0.01 mm. The plate load test was conducted using a loading jack having a ten-ton capacity.

2.1 Sand and Geotextile

The present research used air-dried sand from Nasiriyah city. This sand is categorized as SP by the Unified System of Soil Classification (USCS). Figure 2 depicts the grain-size distribution curve for sand. The relative density of sand in the box was 55% in this research. The physical properties of sand are summarized in Table 1. The parameters of the woven geotextile employed in this investigation are listed in Table 2.

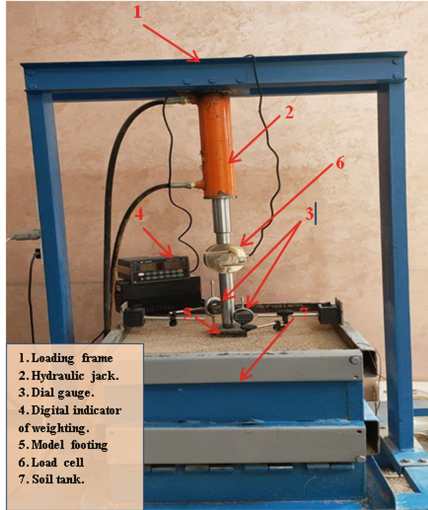


Fig. 1. Configuration of the experiment.

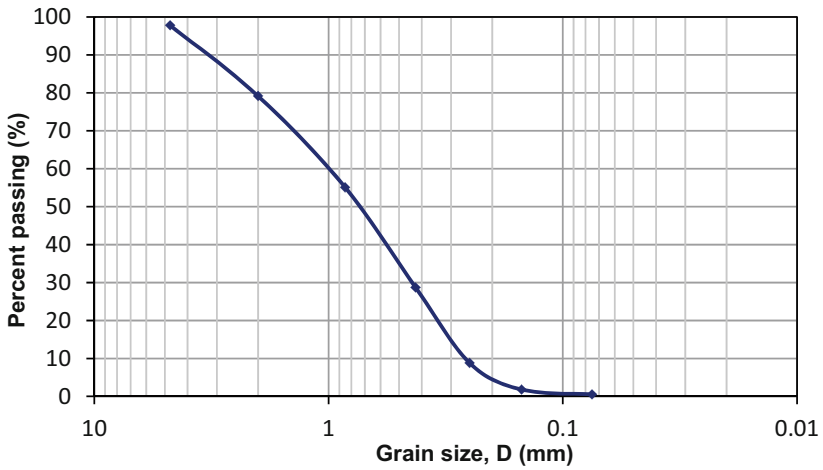


Fig. 2. Distribution of grain sizes of the used soil.

Table 1. Physical characteristics of used sand.

Specific gravity (Gs)	D ₁₀ mm	D ₃₀ mm	D ₆₀ mm	Uniformity coefficient (Cu)	Curvature coefficient (Cc)	Dry unit weight (kN/m ³)		Friction angle (φ)
						Max.	Min.	
2.63	0.26	0.45	1.1	4.23	0.71	18.33	15.2	36.7

Table 2. Properties of geotextile.

Elongation (%)	Tensile strenght (kN/m)	Thick (mm)	Mass (g/m ²)
15.0	80.0	1.10	370.0

2.2 Preparation of Soil Sample

To reach the necessary relative density (55%), Several experiments have been conducted to choose the best technique that compacts soil to a specific density and makes it homogeneous for all the sand. It was shown that utilizing an electrical vibrator may provide a range of relative densities for this kind of sand, ranging from 50% to 95%, depending on the vibration duration. The vibration technique was based on layering the soil in the box then placing a thin steel plate on the surface of each layer to allow the vibrator to move over the entire area of the plate in a specified time, as shown in Fig. 3. Then, gently place another layer of sand and repeat the process until the box is filled with sand. A series of trials were used to calculate the time of vibration required to achieve the required relative density. Densities were measured in each trial by collecting samples in small cans of known volume placed at various places and heights in the test tank.

The relative density in each can was determined using the maximum and minimum densities of the sand. The time needed for vibration to reach 55% relative density was about 25 s. Preparing homogeneous sand layers necessitates increasing the thickness of those layers as the depth of the box increases; therefore, the thicknesses from the bottom to the top layer were (150, 125, 75, and 50) mm, respectively, according to the tests. After completing the sand preparation, care was taken to ensure that the geotextile layers were properly positioned at their specified heights before adding the remaining sand layers. To begin the test, the footing was positioned in the center of the test box. The load on the footing was applied using a hydraulic jack, and load cells having a capacity of 5 tons were used to determine the value. The settlement readings were obtained using an electronic dial gauge. Continuous readings were taken at consistent load intervals till failure.



Fig. 3. Compaction process.

3 Numrrical Modeling

Building various boxes with variable widths and heights is costly; meanwhile, reaching a specific density for bigger containers requires a unique method and considerably more time for each test owing to the enormous quantity of sand. As a result, the 3-D finite element software was utilized to overcome the restriction of conducting plate load tests with multiple boxes of varying sizes. Loading tests on reinforced soil foundations are numerically modeled in this research using the computer software ABAQUS. To simulate both footings and soils, 8-nodded solid elements were used. The footings were square and Linear elastic modeled. The finite element mesh's size was chosen by taking the dimensions of the container and the footing into account in Fig. 4-a. Fixed and rolling boundary conditions were used at the bottom and lateral boundaries, respectively, for the boundary conditions Fig. 4-b. The elastic-perfectly plastic Mohr-Coulomb model was used to simulate soil behavior. The friction angle, cohesion C , and dilatancy angle characterize soil behavior for the Mohr-Coulomb model. The mechanical characteristics of the modeled sand bed are the same as those used in laboratory model loading experiments. Young's sand module was defined using empiric relations representing Young's modulus as a relative density variable [18]. The sand dilation angle (ψ) was also determined according to the empirical relationships for which the internal friction angle is regarded as a function [19] (Table 3).

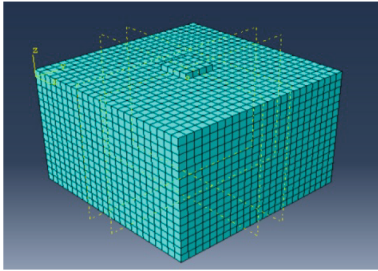
$$E_{\text{sand}} = 25Dr + 20.22 \quad (1)$$

$$\psi = \varphi - 30 \quad (2)$$

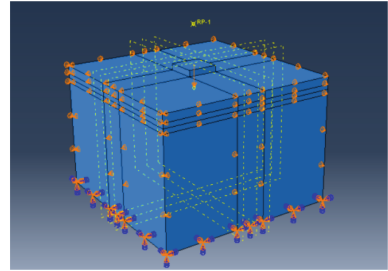
The friction coefficient between the plate and the soil is meaning as ($\eta = \tan\delta$), where (δ) is the interface friction angle. Because the friction angle at the plate soil contact (δ) is dependent on the plate's surface roughness and the soil's effective angle of internal friction, many relationships for various interfaces have been suggested by different researchers [20]. Steel sheet versus clean sand is utilized in [21]. According to this study, In the case of steel sheet versus clean sand, the value of (δ) is 17. For sand, the geotextile–soil interface friction is assumed to be $2/3(\varphi)$. The reinforcement is modeled

Table 3. Material properties used in the analysis.

Material	Cohesion, c (kPa)	Friction, ϕ ($^\circ$)	E (MPa)	ν
Sand	0	36.7	33.97	0.3
Geotextile	500	0.3



(a) Model mesh



(b) Boundary conditions

Fig. 4. 3-D dimensional axisymmetric model utilized in the study.

using the Linear Isotropic model as the material model and the Link 8 element type. The utilized reinforcement has a Poisson’s ratio of 0.3. The ultimate BC was estimated in all finite element analyses as the footing stress associated with a 10% plate width settling. Loads may be applied in infinite element analyses using either controlled displacement or a controlled pressure. The findings of the numerical analyses were verified to those of the laboratory experiment to verify the finite element analysis used in this work.

4 Results and Discussion

4.1 The Influence of the First Geotextile Layer

A one-layered geotextile technique was used to determine the ideal height of the initial geotextile layer (u). To decrease the significance of layer width on achieving the correct height of the first layer, the width of the layer was maintained constant and equal to the width of the container. The stress-settlement curves for foundation tests with a single geotextile layer at varying top layer spacings are shown in Fig. 5. Unreinforced sand has a higher strength than reinforced sand in the initial stages of loading, which may be due to the thinness of the sand layer. It is important to note that the thin sand layer may result in a low effective tension at the sand-geotextile interface and a poor tensile connection between the sand and the geotextile. However, the reinforced sand’s ultimate BC increased with continued loading due to the geotextile’s high tensile strength. According to [22], pressure has a more significant impact on soil strength in less confining environments. Layers with a lower height toward the ground surface, on the other hand, were more successful than layers with a greater height toward the ground surface owing to reduced confining pressure. The differences of bearing capacity ratio (BCR) obtained for various top layer spacing (u) are given in Fig. 6. This Figure demonstrates that as

top layer spacing increases, the BCR values for geotextile reinforced sand generally decrease. Thus, judging from the data, the u/B value of 0.25 seems to be acceptable.

4.2 The Influence of the Geotextile Layer Number

As illustrated in Fig. 7, the optimum number of geotextile layers is computed utilizing the optimum u/B (0.25) value obtained in the previous sections. h/B taken (0.25) [23]. As expected, as the number of reinforcing layers increased, so did the bearing capacity. However, as the number of layers increased, the importance of an extra reinforcing layer decreased. Figure 8 shows the results of models with 1, 2, 3, and 4 layers of geotextile with the comparable nonreinforced model. It is important to note that the final bearing capacity increases as the number of geotextile layers increases, as seen in the Figure. This means that substantial soil movement is required for settlement to occur. As a consequence, soil displacement resistance increases, resulting in less settlement. Figure 8 demonstrates that the BCR increases with N and appears to become virtually constant after ($N = 3$) or has no impact on the soil's ultimate bearing capacity at $0.75B$ depth. Impact depth (d/B) is described as the depth below the foundation at which an extra reinforcing layer substantially contributes to the rise in BCR. Similar to such findings, Guido et al. [24] observed that geogrids and geotextiles below $1.0B$ could not enhance sand bearing capacity. Based on the results of [25], Sakti and Das [26] showed that geotextiles used beneath $1B$ did not improve the bearing capacity of clay. As a result, the ideal number of reinforcements in this investigation was $N = 3$.

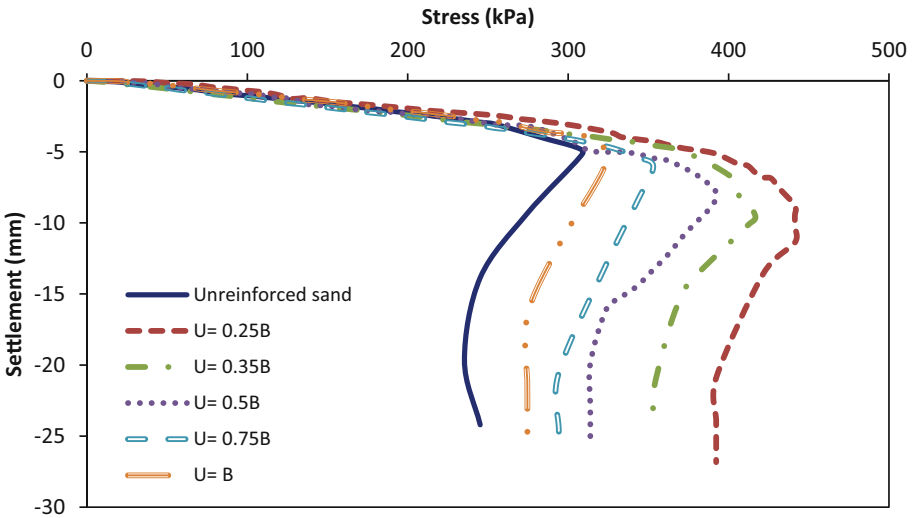


Fig. 5. Stress-settlement curves for model footing tests.

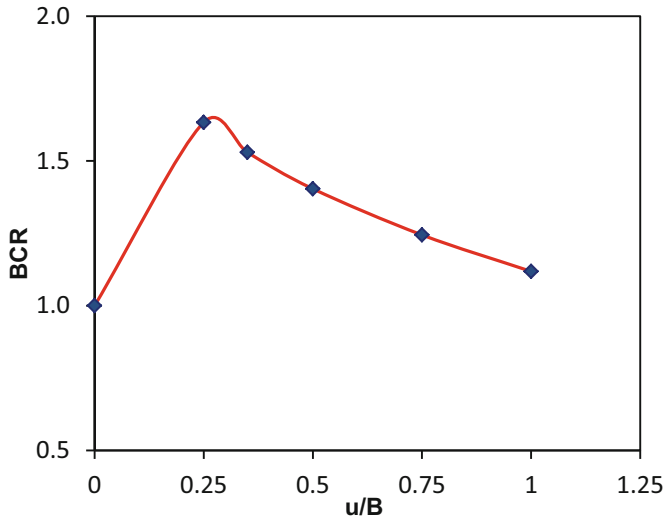


Fig. 6. Relationship between BCR and u/B.

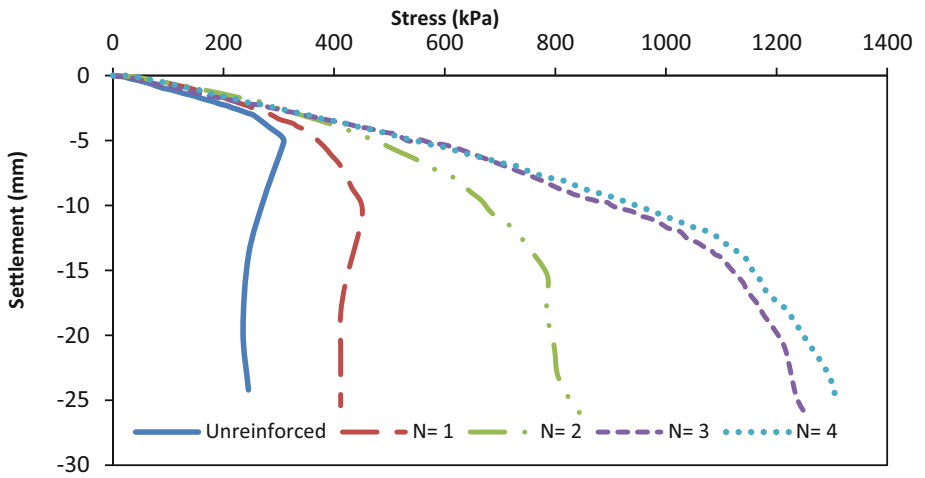


Fig. 7. Stress-settlement curves for varied geotextile layers.

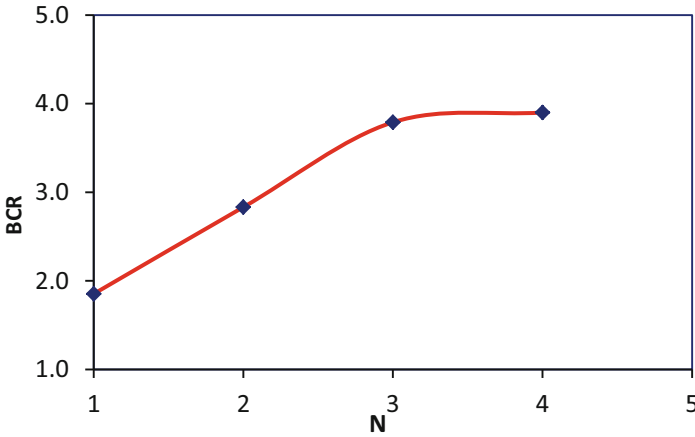


Fig. 8. BCR versus N.

4.3 Finite Element Model Validation

Finite element (FE) studies were compared to the results of experiment model testing for a square foundation on reinforcement to evaluate the appropriateness of the chosen models for the soil, geotextile, and geotextile-soil interaction. The comparison of FE analyses and experiment model testing for unreinforced and three-layer geotextile reinforced sand soil is shown in Fig. 9, which indicates that the similarity between laboratory and numerical results is good.

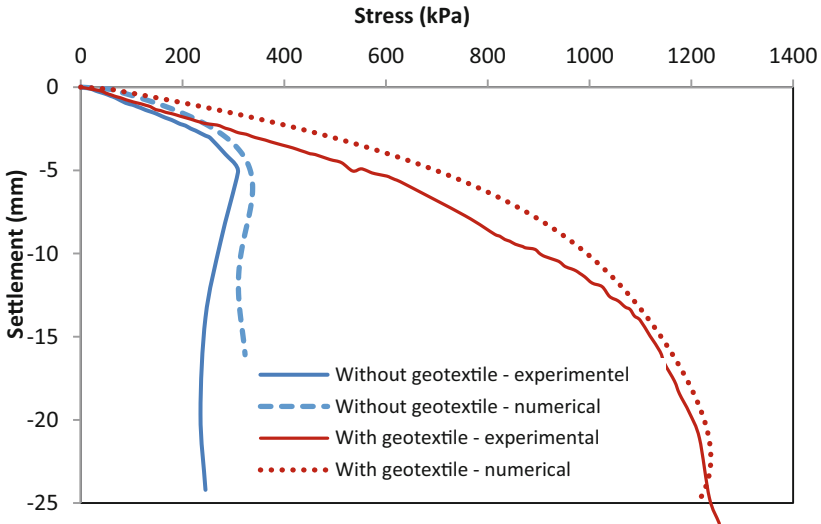


Fig. 9. Comparison of experimental and numerical data

4.4 Scale Effect of Model Testing

Finite elements are initially performed on a 100 mm wide square footing, the same size as laboratory testing. At the next series of FE, the footing size is raised to three times and six times the width of footing used in experimental tests. The same scale factors raise the size of the soil box and reinforcement. All models have the same soil and reinforcing characteristics and maintain the vertical spacing ratio (h/B) and constant reinforcing layers (N). Figure 10 shows that the stress settlement curves of un-reinforced soil for various footings have the same form. This finding indicates that the un-reinforced soil footing has no scale impact in this research if the settlement is represented as a non-dimensional relative settlement of s/B . This numerical finding agrees with the static loading tests performed by [27]. The overall depth ratio of reinforcement (d/B) remains constant across all footing sizes, whereas as the size of the footing rises, so does the vertical spacing of reinforcement. As shown in Fig. 10, As the footing size grows, the BC of reinforced soil with the same settling ratio (s/B) diminishes. The changes in BCR obtained for settling ratio of s/B (10%) for various footing sizes (B) are shown in Fig. 11. As this Figure indicates, the BCR decreases as the footing size increases. The enhanced BCR values associated with smaller plates seem to be connected to the closer distance between geotextile layers and the noticeable influence of confining pressure.

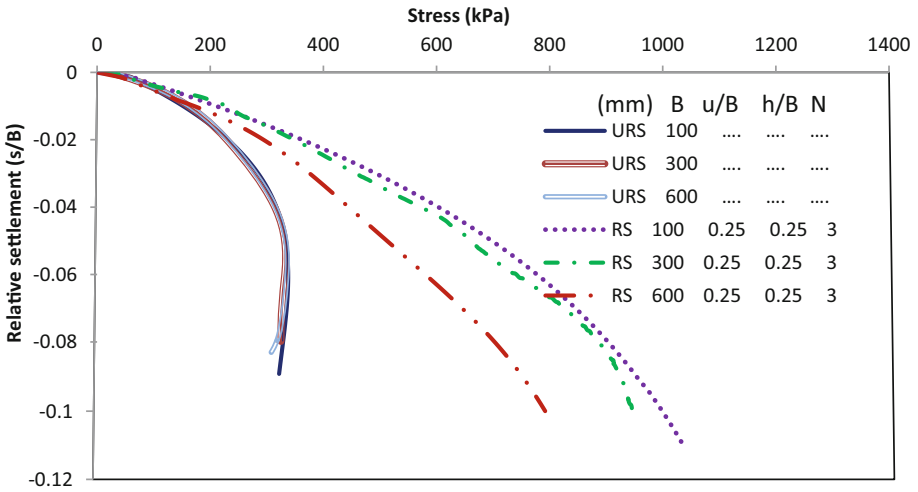


Fig. 10. Stress-settlement curves with different plate size.

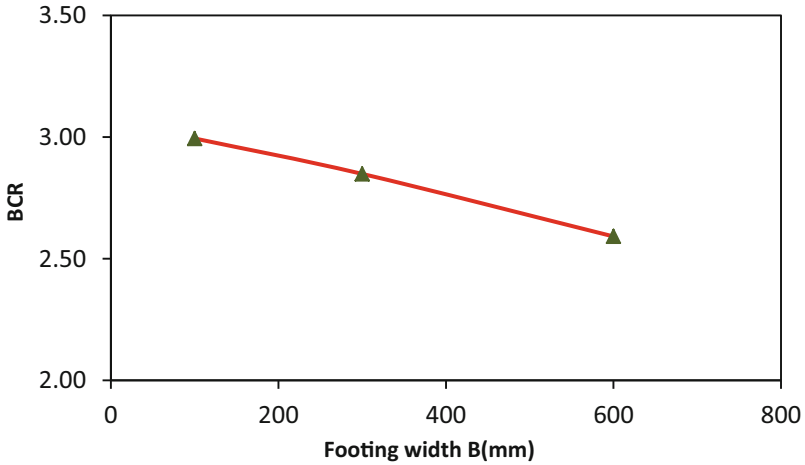


Fig. 11. BCR against the width of footing.

4.5 Thickness of Geotextile

Three FE analyses were performed to examine the impact of geotextile thickness on ultimate bearing capacity response, as illustrated in Fig. 12. For this case, the overall reinforcing depth ratio (d/B), as well as the vertical ratio (h/B) of reinforcing layers, and the number of reinforcing layers N are all kept constant from the experimental test. The geotextile thickness is increased to 2 and 3 from the geotextile thickness used in the practical test (1.1 mm). As a result, thickness of the geotextile increases, so does the bearing capacity of the soil Fig. 12.

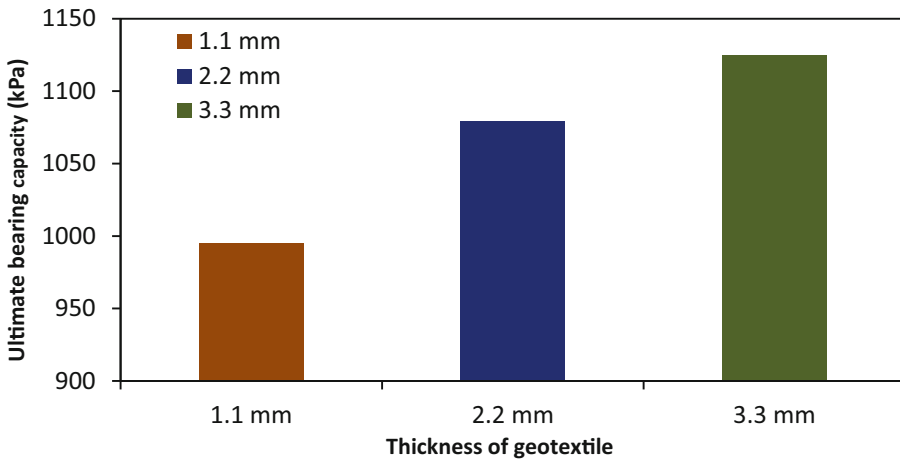


Fig. 12. Thickness of geotextile versus ultimate bearing capacity.

4.6 Sand Overlying Silty Sand Soil

The main objective of these numerical models was to see whether putting a thin layer of sandy soil over silty sand soil would improve the bearing capacity and reduce settlements. Previous investigations were a tool for determining the thickness of a top layer of sand [28]. The sand soil and geotextile properties are the same as those used in the practical study. Table 4 shows the properties of silty sand used in this numerical study based on [29]. Figure 13 depicts the reinforcing plan for two types of soils for square footing. The types of soil and parameters of reinforced soil foundations such as u , h , b , and N may be seen in this diagram. For this research, the following parameters were chosen: $u/B = 0.3$; $h/B = 0.3$; $b/B = 5$, and the number of geotextile layers (N) = 3. The findings demonstrate that using a geotextile-reinforced sand layer over silty sand soil substantially impacts bearing capacity and considerably decreases footing settlement, as illustrated in Fig. 14.

Table 4. Properties of silty sand.

γ (kN/m ³)	Friction angle θ°	Cohesion, c (kPa)	E (MPa)	ν
17.88	28	7.1	30	0.3

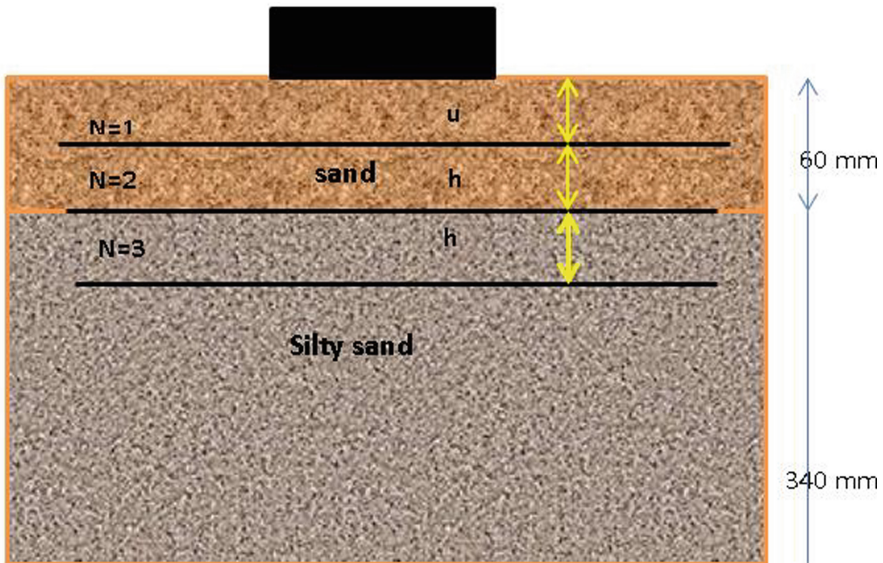


Fig. 13. The arrangement of two kinds of soils.

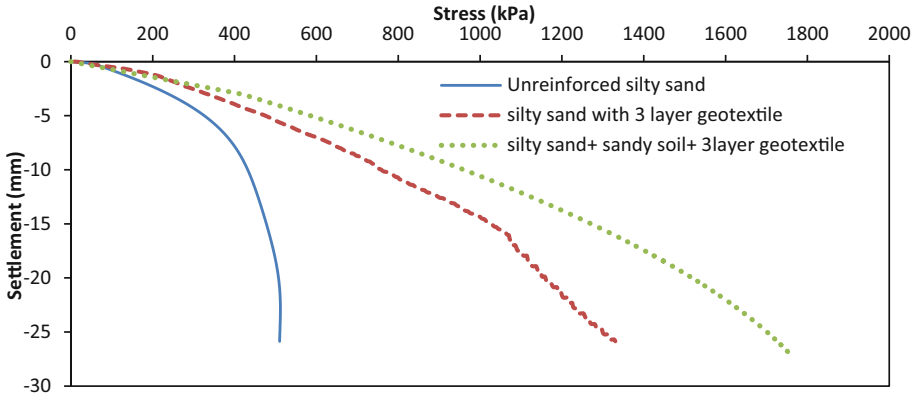


Fig. 14. Stress versus settlement of square footing.

5 Conclusion

The following conclusions about the behavior of a square foundation sitting on sand that has been reinforced with many layers of geotextile may be obtained from experimental data and numerical findings.

- The most significant improvement in maximum load BC comes at a reinforcement height of $0.25 B$.
- The ultimate BC of woven geotextile reinforced soil is calculated using a technique that utilizes three geotextile layers. Using four layers will not show a noticeable improvement than using three.
- If an overall depth ratio of reinforcing d/B , the vertical spacing ratio of reinforcement layers h/B , and the total number of reinforcement layers (N) are held constant. In this situation, as the footing size increases three times and six times from the footing width used in a laboratory test, the BC of reinforced soil decreased to 5.4% and 20%, respectively.
- It can be seen that the BC of the soil increases at rates 8.5% and 13% when using double and triple the original thickness of the geotextile.
- The BC of silty sand soil is increased by adding a thin layer of sandy soil and three layers of geotextile at a rate of 124.5%.

References

1. Adams, M.T., Collin, J.G.: Large model spread footing load tests on geosynthetic reinforced soil foundations. *J. Geotech. Geoenviron. Eng.* **123**(1), 66–72 (1997)
2. Han, J., et al.: Performance of geocell-reinforced RAP bases over weak subgrade under full-scale moving wheel loads. *J. Mater. Civ. Eng.* **23**(11), 1525–1534 (2011)
3. Binquet, J., Lee, K.L.: Bearing capacity tests on reinforced earth slabs. *J. Geotech. Eng. Div.* **101**(12), 1241–1255 (1975)

4. Chen, Q., Abu-Farsakh, M.Y., Sharma, R., Zhang, X.: Laboratory investigation of behavior of foundations on geosynthetic-reinforced clayey soil. *Transp. Res. Rec.* **2004**(1), 28–38 (2007)
5. Rethaliya, R.P., Verma, A.K.: Strip footing on sand overlying soft clay with geotextile interface. *Indian Geotech. J.* **39**(3), 271–287 (2009)
6. Kolay, P.K., Kumar, S., Tiwari, D.: Improvement of bearing capacity of shallow foundation on geogrid reinforced silty clay and sand. *J. Constr. Eng.* **2013**, 1–10 (2013)
7. Demir, A., Yildiz, A., Laman, M., Ornek, M.: Experimental and numerical analyses of circular footing on geogrid-reinforced granular fill underlain by soft clay. *Acta Geotech.* **9**(4), 711–723 (2013). <https://doi.org/10.1007/s11440-013-0207-x>
8. Karkush, M.O., Yassin, S.: Improvement of geotechnical properties of cohesive soil using crushed concrete. *Civ. Eng. J.* **5**(10), 2110–2119 (2019)
9. Karkush, M.O., Ali, H.A., Ahmed, B.A.: Improvement of unconfined compressive strength of soft clay by grouting gel and silica fume. In: Wu, W., Yu, H.-S. (eds.) *Proceedings of China-Europe Conference on Geotechnical Engineering*. SSGG, pp. 546–550. Springer, Cham (2018). https://doi.org/10.1007/978-3-319-97112-4_122
10. Karkush, M., Jabbar, A.: An improvement of bearing capacity of soft soil and reducing excess porewater pressure using several patterns of floating stone columns. *J. Eng. Res.* (2021)
11. Yetimoglu, T., Wu, J.T., Saglamer, A.: Bearing capacity of rectangular footings on geogrid-reinforced sand. *J. Geotech. Eng.* **120**(12), 2083–2099 (1994)
12. Sitharam, T.G., Sireesh, S.: Model studies of embedded circular footing on geogrid-reinforced sand beds. *Proc. Inst. Civ. Eng.-Ground Improv.* **8**(2), 69–75 (2004)
13. Latha, G.M., Somwanshi, A.: Bearing capacity of square footings on geosynthetic reinforced sand. *Geotext. Geomembr.* **27**(4), 281–294 (2009)
14. Abu-Farsakh, M., Chen, Q., Sharma, R.: An experimental evaluation of the behavior of footings on geosynthetic-reinforced sand. *Soils Found.* **53**(2), 335–348 (2013)
15. Kazi, M., Shukla, S.K., Habibi, D.: An improved method to increase the load-bearing capacity of strip footing resting on geotextile-reinforced sand bed. *Indian Geotech. J.* **45**(1), 98–109 (2015)
16. Tavangar, Y., Shooshpasha, I.: Experimental and numerical study of bearing capacity and effect of specimen size on uniform sand with medium density, reinforced with nonwoven geotextile. *Arab. J. Sci. Eng.* **41**(10), 4127–4137 (2016)
17. Panigrahi, B., Pradhan, P.K.: Improvement of bearing capacity of soil by using natural geotextile. *Int. J. Geo-Eng.* **10**(1), 1–12 (2019). <https://doi.org/10.1186/s40703-019-0105-7>
18. Al-Defae, A.H., Caucis, K., Knappett, J.A.: Aftershocks and the whole-life seismic performance of granular slopes. *Géotechnique* **63**(14), 1230–1244 (2013)
19. Chae, K.S., Ugai, K., Wakai, A.: Lateral resistance of short single piles and pile groups located near slopes. *Int. J. Geomech.* **4**(2), 93–103 (2004)
20. Shooshpasha, I., Amirdehi, H.A.: Evaluating the stability of slope reinforced with one row of free head piles. *Arab. J. Geosci.* **8**(4), 2131–2141 (2014). <https://doi.org/10.1007/s12517-014-1272-7>
21. U.S. Navy: *Foundations and earth structures design manual 7.2*. Department of the Navy, Navy Facilities Engineering Command, Alexandria, Va (1982)
22. Haeri, S.M., Noorzad, R., Oskoorouchi, A.M.: Effect of geotextile reinforcement on the mechanical behavior of sand. *Geotext. Geomembr.* **18**(6), 385–402 (2000)
23. Thamer, L., Shaia, H.: The effect of geotextile layers and configuration on soil bearing capacity. *Math. Model. Eng. Probl.* **8**(6), 897–904 (2021)
24. Guido, V.A., Chang, D.K., Sweeney, M.A.: Comparison of geogrid and geotextile reinforced earth slabs. *Can. Geotech. J.* **23**(4), 435–440 (1986)
25. Omar, M.T., Das, B.M., Puri, V.K., Yen, S.C.: Ultimate bearing capacity of shallow foundations on sand with geogrid reinforcement. *Can. Geotech. J.* **30**(3), 545–549 (1993)

26. Sakti, J.P., Das, B.M.: Model tests for strip foundation on clay reinforced with geotextile layers. *Transportation Research Record*, (1153) (1987)
27. Chen, Q.: An experimental study on characteristics and behavior of reinforced soil foundation (2007)
28. Khing, K.H., Das, B.M., Puri, V.K., Yen, S.C., Cook, E.E.: Foundation on strong sand underlain by weak clay with geogrid at the interface. *Geotext. Geomembr.* **13**(3), 199–206 (1994)
29. Arora, M., Dutta, R.K., Soni, D.K.: Bearing ratio behavior of sand overlying silty sand and reinforced with treated coir geotextiles. *J. Nat. Fibers* **18**(6), 834–844 (2021)